Algorithm Theoretical Basis Document (ATBD) for Deep Convective Cloud (DCC) technique of calibrating GEO sensors with Aqua-MODIS for GSICS

David Doelling[1], Dan Morstad[2] ,Rajendra Bhatt[2], Benjamin Scarino[2]
[1]NASA-Langley, [2]SSAI
August 19, 2011

Introduction

The DCC technique is an invariant target calibration approach designed to verify the stability of the GEO calibration. Other invariant targets include earth targets, such as the deserts and clear-sky ocean, or non-earth targets such as the sun and the moon. The advantage of using DCC is that they are available over all GEO domains. They are at the tropopause level, therefore the effects of atmospheric absorption are reduced with the exception of stratospheric aerosols, and they are the brightest targets on earth - a combination of highly reflective clouds at near nadir solar angles. DCC are solar diffusers, which have predictable, near Lambertion albedos.

The ATBD DCC calibration technique proposed for GSICS follows the approach outlined in Morstad et al. 2011. The first DCC calibration approach was used to validate the CERES fluxes on the TRMM and Terra satellites (Hu et al. 2004). He also evaluated the stability of the VIRS and Terra-MODIS imagers during 2000 to 2002. Shortly thereafter DCC calibration was demonstrated using AVHRR (Doelling et al. 2004). Minnis et al. 2007 used DCC to assess the operational calibration of VIRS and Terra-MODIS. It is worth noting that over the last 20 years, there have been a variety of calibration approaches that depend on bright clouds (Vermote and Kaufmann 1994, & Govaerts et al. 2001). Sohn et al. 2009 used a theoretical model, based on MODIS cloud properties, to predict the sparsely identified DCC pixel level radiances. The success of this technique relies on a large ensemble of identified DCC pixels. The DCC identification is dependent on the IR temperature, and visible and IR pixel level homogeneity thresholds. This technique requires good IR and visible co-registration, IR calibration, and a visible dynamic range that does not saturate at DCC radiances. The lower the IR threshold the greater the chance of identifying DCC rather than anvil conditions, however, it is at the expense of DCC sample size. The DCC radiances are converted to nadir viewing and solar conditions using an empirical DCC model. The sampled nadir DCC radiances provide a monthly Probability Density Function (PDF), the mode of which is used to track the DCC radiance over time. In a perfect observing system the DCC nadir radiances are expected to be constant over time.

A reference sensor is required for absolute calibration transfer. It has been determined that the Aqua-MODIS instrument is better characterized and more stable than Terra-MODIS, and, therefore, is the calibration standard for GSICS. The Aqua-MODIS calibration can easily be adjusted if another reference sensor is agreed upon or if stability adjustments are needed. The nadir Aqua-MODIS DCC radiance over the lifetime of Aqua is the absolute DCC reference radiance that can be applied to the target sensor. The spectral difference between the reference and target sensor is based on hyper-spectral

SCIAMACHY DCC footprint radiances. There are known geographical and IR threshold dependencies on the absolute nadir DCC MODIS radiances (Doelling et al. 2010). However, the GEO DCC criterion has been carefully selected so that both Aqua-MODIS and the target GEO are observing the same DCC. Once the DCC criteria are established over a GEO domain, the DCC nadir radiances are very stable being that these dependencies do not change in time.

The Global Space-based Inter-Calibration System (GSICS) aims to inter-calibrate a diverse range of satellite instruments in order to produce corrections that ensure their data are consistent, thereby allowing them to be used to produce globally homogeneous products for environmental monitoring. Although these instruments operate on different technologies for different applications, their inter-calibration can be based on common principles: Observations are collocated, transformed, compared, and analyzed to produce calibration correction functions - transforming the observations to common references. To ensure the maximum consistency and traceability, it is desirable to base all the inter-calibration algorithms on common principles, following a hierarchical approach, described here. The algorithm is defined in 3 generic steps:

1. Identifying DCC pixels
2. Spectral, angular and PDF transformation of the data
3. Monthly visible gain computation and temporal gain monitoring

The ATBD also includes an uncertainty analysis. This ATBD provides the methodology for GEO and LEO DCC calibration

1. Identifying DCC pixels

To transfer the Aqua-MODIS calibration successfully the GEO DCC identification criteria should capture the same DCC that Aqua observes. The DCC domain is confined to ± 20°N for GEO and LEO satellites. The GEO longitude domains are given in Table 2. Most DCC are located within the Intertropical Convergence Zone (ITCZ) near the equator. The ITCZ has a pronounced seasonal cycle, and the DCC domain should encompass the seasonal extent. Five GEO images surrounding the local equator crossing time of the reference sensor Aqua-MODIS is adequate. Nominal pixel resolution of ~4 km for GEO is sufficient. Both visible and IR pixels must have the same resolution.

For this technique, DCC are identified as any pixel with 11-μm brightness temperatures less than 205° K. Although the GEO satellites have IR onboard calibration using blackbodies, which can be corrected to the GSICS based IASI calibration, the IR temperature needs to match the Aqua-MODIS 11μm (band 31) temperature, since that was the basis of the IR threshold used to identify DCC for Aqua-MODIS. In Figure 1a and 1b, a ray-match of GOES-13 and Aqua-MODIS $BT_{11\mu m}$ shows that a daytime bias (GOES – MODIS) of approximately 1.5° K exists at 205° K. For convenience these temperature differences for the current GEO operational satellite have been listed in Table 2. It is anticipated in future ATBD's the GSICS IR corrections will be applied to both MODIS and GEO making this step unnecessary.
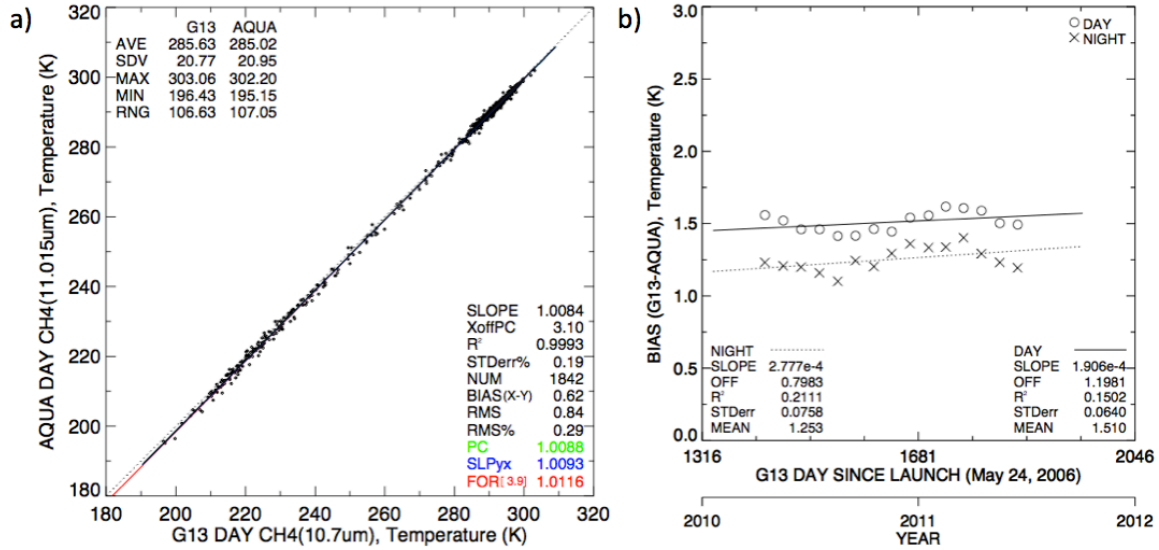
Figure 1: a) Ray-match results for Aqua-MODIS to GOES-13 inter-calibration of the $BT_{11\mu m}$ during April 2010 show a potential bias between the GOES-13 and the Aqua-MODIS brightness temperatures. b) Lifetime trend of the GOES-13 minus Aqua-MODIS $BT_{11\mu m}$ bias at 205° K showing a 1.5° K bias during the daytime ray-matches.

The DCC convective core is the most reflective portion of the cloud and is best suited for transferring calibration. DCC cloud edges and anvils should be avoided. Visible and IR uniformity thresholds are applied to avoid cloud edges. The IR temperature and visible standard deviation are computed using 3 x 3 pixel blocks, and are limited to less than 1° K and 3% of the visible mean respectively. These general thresholds were empirically derived and are applicable to most GEO satellite imagers. The DCC thresholds are summarized in Table 1. Figure 2 highlights the DCC identified pixels for a GOES-12 image.

GEO Parameters	DCC threshold
Latitude Geographical extent	20°N to 20°S all surface types
Longitude Geographical extent	±20° E/W of GEO sub-satellite (see Table 2)
Solar Zenith Angle	SZA<40°
View Zenith Angle	VZA<40°
Window Brightness Temperature	$BT_{11\mu m}$ < Aqua-MODIS 205°K (see Table 2)
Brightness Temperature Homogeneity	Standard deviation $BT_{11\mu m}$ < 1°K
Visible Radiance Homogeneity	Standard deviation $R_{0.6\mu m}$<3%
Local Time range at GEO subsat longitude	12:00PM<image time<3:00PM (see Table 2)

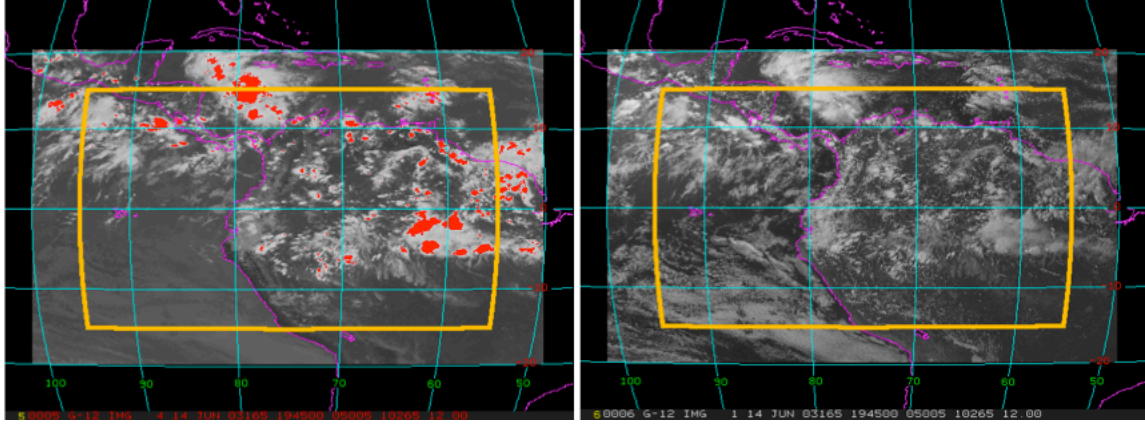Table 1 Summary of the GEO DCC thresholds used in this ATBD

Figure 2: Left panel) GOES-12 10.8-µm IR brightness temperature image for June 14, 2003 at 19:45 GMT. The red pixels depict pixels with an IR temperature < 205 K. Right panel) is the corresponding visible image. The yellow box does not define the GOES-12 GEO domain.

2. Spectral, angular and PDF transformation of data

In this step, valid DCC pixels are transformed to allow their direct comparison at an overhead-sun representation. This includes accounting for solar/viewing geometry effects, and spectral differences between the monitoring and reference sensor. The overhead sun radiances are placed in a probability distribution function to identify the peak radiance. The output radiances of this step are the best estimates of the spectral-band-adjusted DCC-pixel overhead sun response.

2a. Spectral transformation of data

Although DCC are rather spectrally flat in the visible spectrum, differences in spectral response functions (SRF) between the reference and monitoring sensor can introduce a significant error to the inter-calibration. The SRF differences can be accounted for by developing spectral band adjustment factors (SBAF) using SCIAMACHY hyper-spectral data. Deep convective cloud hyper-spectral data acquired over the GEO DCC calibration domain by the SCIAMACHY sensor onboard ENVISAT are used to derive the spectral footprint of the target. The calibrated hyper-spectral at-sensor radiances from SCIAMACHY are then convolved with the SRFs of both the geostationary and MODIS channels to estimate the Spectral Band Adjustment Factor (SBAF) for an individual GEO-AQUA pair using Equation 1 and is described in Doelling et al. 2011a.

$$ SBAF = \frac{\int R_{GEO}(\lambda).\rho_{SCIA}(\lambda)d\lambda / \int R_{GEO}(\lambda)d\lambda}{\int R_{AQUA}(\lambda).\rho_{SCIA}(\lambda)d\lambda / \int R_{AQUA}(\lambda)d\lambda} . \quad (1) $$

Figure 3 shows the SCIAMACHY pseudo DCC footprint radiances between GOES-12 and Aqua-MODIS derived from 5 years of seasonal months from 2003-2007. The DCC spectral reflectance is very linear in the visible owing to the absence of water vapor absorption originating from the troposphere. This fact ensures that the DCC spectral

correction is small between the two sensors. The linear regression through the origin is used to compute SBAF. The current GEO SBAF adjustments are given in Table 3. For a given reference sensor and monitoring sensor, the radiance measured by the monitoring sensor is related to that of the other by the SBAF if both are perfectly calibrated. The *SBAF* is simply the ratio of the imager pair pseudo-radiances, which are the convolved radiances $L_{Monitoring}$ and $L_{Reference}$ from the SCIAMACHY data and are applied as shown in Eq. 2,
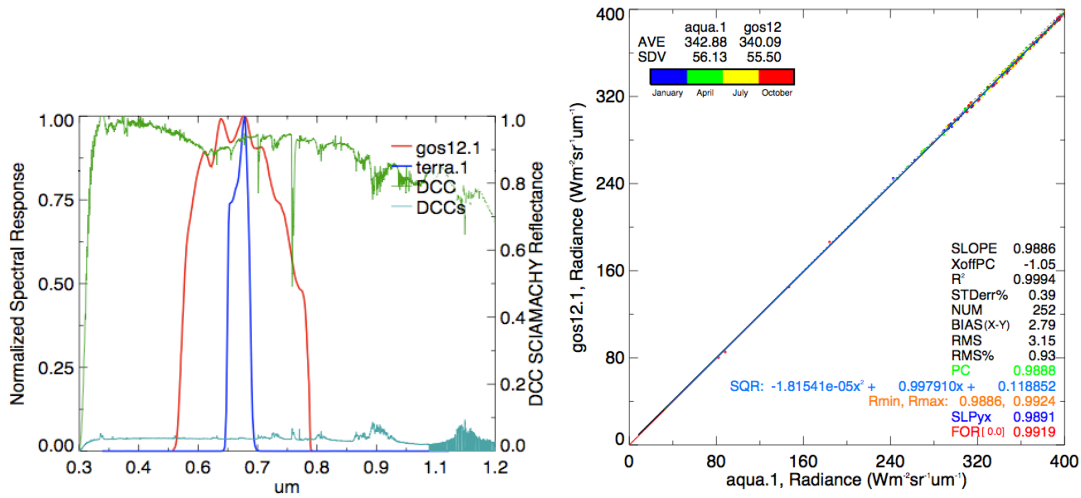
$$L_{Monitoring} = SBAF \ x \ L_{Reference}. \tag{2}$$

Figure 3: Left panel) GOES-12 and Terra-MODIS 0.65-µm SRFs overlaid on the SCIAMACHY DCC mean reflectance spectra in green with standard deviation in dark green. Right panel) Scatter plot of SCIAMACHY footprint pseudo Aqua-MODIS and GOES-12 0.65-µm DCC radiance pairs over the GEO DCC domain.

2b. Angular transformation of data

Differences in viewing/solar geometry will lead to differences in DCC response if these angular configurations are not normalized to a uniform set. This portion of the algorithm normalizes each of the spectrally corrected DCC pixels to an overhead-sun NADIR-looking configuration. When this normalization is identical between the reference and the monitoring sensors, a direct inter-calibration can be completed. The CERES Angular Distribution Model (ADM) (available at http://asd-www.larc.nasa.gov/Inversion/adm/adm.html) for overcast ice clouds with optical depths of 50 or greater is then applied to the radiance in order to remove any anisotropy present in the DCC response. The CERES ADM (Loeb et al 2003) was empirically modeled from the 10-km CERES footprint broadband radiances, when the CERES instrument was in rotating-azimuth plane-scan mode, which samples all viewing and azimuthal conditions. The model was derived from CERES radiances onboard the TRMM spacecraft, which precessed through all solar zenith angles every 23 days. The cloud properties for the radiances were derived from coincident VIRS imager cloud retrievals. The CERES DCC albedos (ALB) then convert the nadir radiance to overhead sun conditions. It is preferable to limit the solar and view angles within 40°, where DCC are most isotropic as indicated

by the ADM (recapped in Table 1). For narrowband imagers, it has been empirically determined that the CERES broadband ADM is unreliable for solar zenith angles greater than 55°. Equation 3 relates the DCC observed radiance to a nadir radiance. The d^2 term is the earth-sun distance correction factor, whereas sz, vz, and az refer to the solar zenith, view zenith and relative azimuth angles.

$$rad_{nadir}^{DCC} = \frac{rad_{sz,vz,az}^{DCC} ALB_{sz=0}^{DCC}}{d^2 \cos(sz) ADM_{sz,vz,az}^{DCC} ALB_{sz}^{DCC}}$$ (3)

2c. PDF transformation of data

Individual pixel DCC nadir radiance error could potentially affect a calibration of the monitoring sensor if an inadequate sample size of DCC pixels were identified. For this reason, we choose to compile all DCC pixels within a month and generate a probability distribution function (PDF) of the pixels. In order to compute the monthly gain, DCC nadir counts, which are proportional to radiance, are used to create the PDF. It is important to remove the space count offset, and to properly adjust the DCC count, to account for the detector response, whether it is linear or squared before deriving the PDF. The rad term in equation 3 can then be replaced by the count relationship that is proportional to radiance. The success of this method is to identify enough DCC pixels thereby allowing for PDF shapes that are very smooth and similar from month to month. Figure 4 shows the time sequence of monthly PDFs. Note that as the GOES-12 visible calibration degrades over time, the mode migrates to the left of the plot.
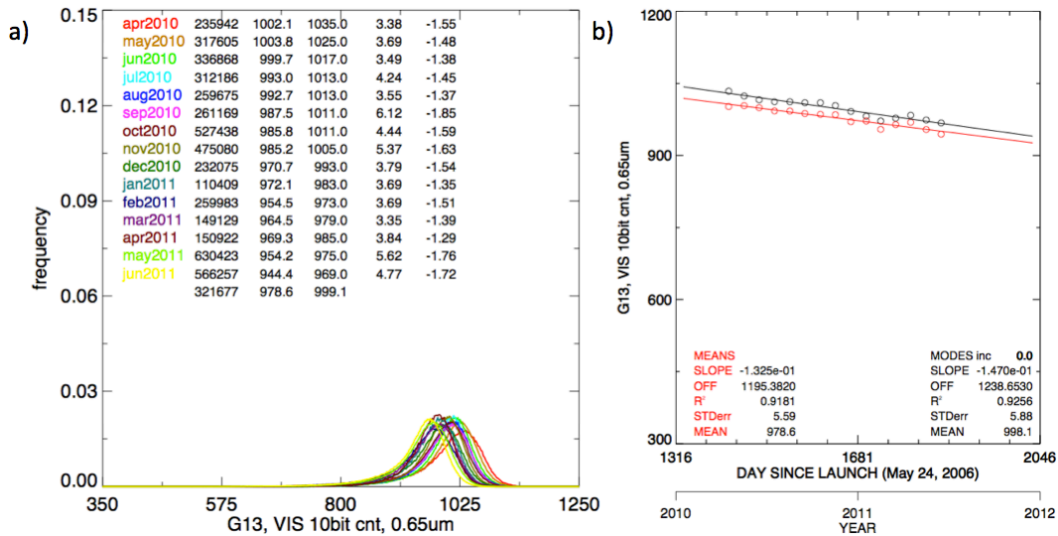

Figure 4: a) DCC PDFs throughout the lifetime of GOES-13 showing sensor degradation of the DCC nadir visible counts. b) GOES-13 DCC mode and mean trends show a linear degradation of the visible counts observed for DCC at local noon in the GOES-13 domain.

Insufficient DCC pixels usually manifest as noisy PDFs, where the mode is not easily identifiable. Over most GEO domains the monthly DCC pixel count is greater than 100K. Noisy PDFs are avoided by relaxing the DCC thresholds, increasing the PDF bin

resolution or acquiring more GEO images. Typical count PDF bin resolutions are given in Table 2. Further filtering of the DCC pixel level data may be implemented to improve the signal to noise ratio by sharpening the peak of the PDF. Filtering includes the IR threshold temperature, spatial visible and IR homogeneity tests, and PDF bin resolution. It is preferable to have a year's worth of data before finalizing the constraints because of the seasonal variation of the monthly gains derived from GEO DCC calibration.

3. Monthly visible gain computation and temporal gain monitoring

3a. Monthly visible gain computation

DCC cloud edges and anvils typically manifest in the forms of tails on the PDF. These tails have less of an effect on the mode statistic; therefore, the mode statistic is superior to the mean statistic for performing inter-calibrations.

Aqua-MODIS DCC response has stayed nearly constant over time, signifying a very stable sensor (Doelling et al. 2010). The Aqua-MODIS analysis follows the same procedure as outlined in this ATBD with the only difference being that the MODIS Level-1B radiance data were used instead of raw counts. This results in a PDF of calibrated radiances that can be directly used for inter-calibration of the monitoring sensor. Given that Aqua-MODIS is the GSICS reference sensor, the average mode for all 9-years of the monthly PDFs over the GEO domain can be taken to be the true overhead-sun/NADIR-viewing radiance. These DCC overhead radiances have been computed for various GEO domains in as shown in Table 3.

The GEO monthly gain is then derived using Equation 4 for detectors that have a linear response. For squared count detector response is simply the square of the value inside the parenthesis.

$$Aqua_{DCCradiance}^{nadir}SBAF_{GEO/Aqua} = Gain_{GEO}\left(CNT_{DCC \bmod e}^{nadir} - CNT_{space}\right)$$

(4)

GEO satellite	Aqua-GEO IR (K) difference	Domain longitude	GMT image range	PDF count increment
FY2E	-0.55	85°E to 125°E	5:00 to 8:00	
GOES-11	-1.23	155°W to 115°W	21:00 to 24:00	
GOES-13	-1.15	95°W to 55°W	17:15 to 19:45	
MTSAT-1	0.11	120°E to 160°E	2:30 to 5:30	
MET-7	-2.38	37°E to 77°E	8:00-11:00	
MET-9	0.22	20°W to 20°E	12:00 to 15:00	

Table 2: Summary of GEO DCC parameters.

3b. Temporal gain monitoring

In order to monitor the GEO sensor gain over time, the computed monthly gains are plotted as a function of time to get a lifetime sensor calibration (Figure 5). The time is measured in days since launch (DSL). The trend line for GEO-sensor gain is derived from an appropriate fit to the data. A fitted model (linear, exponential, polynomial, etc)

can then be used to represent the calibration. The GOES-13 DCC calibration is compared with ray-matching and desert calibration in figure 5 right panel. The resultant GOES-13 absolute calibrations are within 1.4%, based on the 15-month gain means, indicating the robustness of the DCC technique (Morstad et al. 2011). At least 3-years of monthly means are needed to assess the trend consistency.
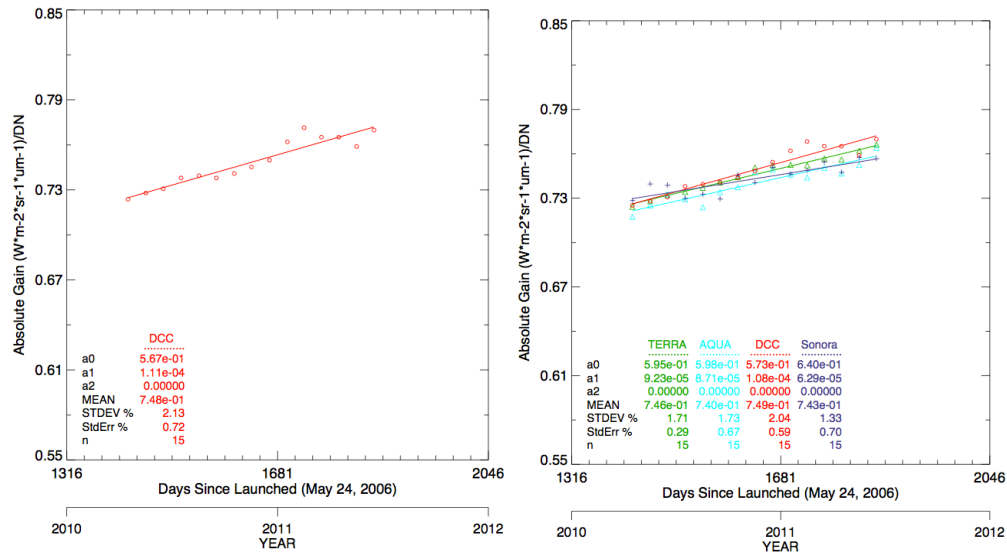

Figure 5: Shows monthly DCC mode gains for GOES-13 as a function of time. Right plot) shows the GOES-13 monthly gains based on ray-matching, desert and DCC approaches.

Uncertainty analysis

The GEO DCC calibration uncertainty can be divided into four components: the Aqua-MODIS calibration, DCC calibration technique, DCC calibration transfer, and the DCC spectral correction.

The Aqua-MODIS absolute calibration band 1 (0.65 µm) uncertainty at covers-open after launch is 1.64% (Xiong 2011). The Aqua-MODIS stability is 0.2±0.9%/decade (2 sigma) for the nadir scan position. This ray-matching domain confines the MODIS radiances to be near nadir.

The DCC calibration technique has been shown to assess the stability of well-calibrated sensors (Minnis et al. 2007). The DCC calibration technique is only as good as the invariant DCC earth targets. Doelling et al. 2011b showed for visible channels with a spectral range less than 1µm that the seasonal and inter-annual DCC nadir radiance variability is less than 1%, based on the mean statistic. The mode statistic is predicted to have a smaller variability (Morstad et al. 2011). The uncertainty of the DCC calibration technique is the combined uncertainty of the stability of the target and the methodology described above. The standard error of the monthly DCC gains over time is the best indicator of the uncertainty for the technique. These are a given as a function of GEO domain and given in Table 3.

The DCC calibration transfer uncertainty is based on how well the GEO and reference sensor observe the same population of DCC. Doelling et al. 2010 indicated geographical variations of the DCC nadir radiance using the mode statistic over the tropics and that there is slight a dependency of the IR threshold temperature on the DCC nadir radiance. Morstad et al. 2011 compared multiple Aqua-MODIS to GOES-13 calibration transfer approaches using the global versus GOES-13 domain Aqua DCC nadir radiance, using GOES-13 noon versus 1:30PM images, and using a GOES-13 IR threshold temperature of 205°K versus 206.5°K. It was found that the greatest absolute calibration difference was ~1.2% for all these comparisons when using the mode statistic. However using the Aqua-MODIS equivalent IR temperature threshold, the GEO domain, and Aqua overpass GEO image times should reduce the uncertainty in the Aqua-MODIS to GEO calibration transfer using the DCC calibration technique.

GEO satellite	Aqua DCC radiance $(Wm^{-2}sr^{-1}\mu m^{-1})$	Trend Standard Error (%)	GEO/Aqua-MODIS SBAF correction (radiance/reflectance)	SBAF Standard Error (%)
FY2E		1.1	0.855/0.996	0.77
GOES-11		0.7	0.977/0.991	0.35
GOES-13	719.1	0.7	1.041/0.998	0.25
MTSAT-1		3.5	0.856/0.995	0.78
MET-7		1.0	0.873/0.994	0.59
MET-9		0.7	1.017/0.9962	0.07

Table 3: DCC and spectral correction uncertainty analysis.

The spectral correction uncertainty is based on the pseudo, SCIAMACHY-derived, MODIS and GEO radiances. It is not known if there is color dependency of the GEO SRF degradation over time. Based on MODIS and CERES experience, the blue portion of the spectrum will degrade faster than the longer wavelengths for low earth orbits. For this error analysis, the GEO SRF is assumed to be perfect, and there is no change over time. The MODIS SRF is well monitored and the temporal variations have been small (Xiong 2011). The DCC spectral correction based on SCIAMACHY radiances pairs is quite linear, and the standard error of the regression is a good estimate of the spectral correction uncertainty. Since DCC tops are at tropopause level, there is little water vapor absorption over the DCC spectra as shown in the Figure 3 left panel. The minor regression noise is due to ozone, oxygen, and other gaseous absorption variation between bands. Although the SCIAMACHY DCC identification is less restrictive and footprint size much larger than for an imager, the regression standard error is none the less very small, and the error would be smaller if SCIAMACHY had the footprint of an imager.

The SCIAMACHY stability over time is based on the solar diffuser and assumed to be stable. The absolute calibration of SCIAMACHY is a function of wavelength and given in Table 4. It is not known how the various band uncertainties affect the overall spectra; however, the discontinuities in the overlap regions were small. Absolute calibration is not necessary as long as the band calibration is maintained over time.

Band #	1	2	3	4	5
Band range (μm)	240-314	309-405	394-620	604-805	785-1050

Uncertainty (%)	3	4	3	2	6

Table 4: SCIAMACHY version 7.03 reflectance absolute calibration uncertainty as a function of band, from envisat.esa.int/handbooks/.../disclaimers/SCI_NL__1P_Disclaimers.pdf.

To compute the solar constants from the GEO SRF the solar incoming spectra is required. This is not a concern if the DCC calibration is being performed in reflectance units, only if radiance is desired. The CEOS community has chosen the Thuillier solar irradiance spectra. MODIS radiances use Thuillier solar irradiance spectra from 0.4µm to 0.8µm and Neckel and Labs from 0.8µm to 1.1µm (Xiong 2011). For the uncertainty in the solar incoming spectra, the standard deviation of the convolved visible solar constant from six solar incoming spectral datasets was computed. The datasets include Iqbal (1983), Wherli (1985), Kurucz (2001), Thuillier (2003), Neckel & Labs and a "quiet" (least absorbing) solar spectra from SORCE Spectral Irradiance Monitor (SIM), recommended by Greg Kopp (personal communication 2011). Thekeakara was not used in the analysis being that it was considered an outlier in the spectra between 0.3 and 1.0 µm. Table 5 illustrates the uncertainty in the solar constant based on the variability between spectra from six different sources. The narrowest bands have the greatest uncertainties.

Satellite band	Aqua 0.65µm	Met-7 visible	Met-9 0.65µm	Met-9 0.86µm	GOES-11	MTSAT-1
Uncertainty (%)	1.04	0.55	0.98	1.06	0.68	0.84

Table 5: Solar constant uncertainties based on the standard deviation of six datasets of solar spectra (see text).

To compute the overall uncertainty of the DCC technique for a given GEO/MODIS satellite pair, one would require the combination of the Aqua-MODIS absolute calibration uncertainty, the DCC gain trend-line standard error, the calibration transfer uncertainty and the SCIAMACHY-based SBAF standard error. Table 6 shows the uncertainty calculation for GOES-13.

GEO satellite	Aqua-MODIS (%)	Calibration transfer (%)	Trend (%)	SBAF (%)	Total uncertainty (%)
GOES-13	1.64	1.2	0.7	0.25	2.2

Table 6: The uncertainty analysis for GOES-13 following the approach in this ATBD.

References

Doelling, D. R., C Lukashin, P. Minnis, B. Scarino, D. Morstad, 2011a: Spectral reflectance corrections for satellite intercalibrations using SCIAMACHY data. *Geoscience and Remote Sensing Letters, accepted June 2011*

Doelling et al, 2011b: One the use of Deep Convective Clouds (DCC) to calibrate visible sensors. *GISCS GWRG meeting*, Daejon, Korea, March 22-25, 2011. https://gsics.nesdis.noaa.gov/wiki/Development/20110322

Doelling, D. R. , Gang Hong, Dan Morstad, Rajendra Bhatt, Arun Gopalan and Xiaoxiong Xiong, "The characterization of deep convective cloud albedo as a calibration

target using MODIS reflectances", Proc. SPIE 7862, 78620I (2010); doi:10.1117/12.869577

Doelling, D. R., L. Nguyen, and P. Minnis, 2004: On the use of deep convective clouds to calibrate AVHRR data. *Proc. SPIE 49th Ann. Mtg., Earth Observing Systems IX Conf., Denver, Colorado, August 2-6, 2004*

Govaerts, Y. M., A. Arriaga, and J. Schmetz, "Operational vicarious calibration of the MSG/SEVIRI solar channels", *Adv. Space Res.*, vol. 28, pp.21 -30 2001

Hu, Y., B. A. Wielicki, P. Yang, P. W. Stackhouse Jr., B. Lin, and D. F. Young, 2004: Application of deep convective cloud albedo observation to satellite-based study of the terrestrial atmosphere: Monitoring the stability of spaceborne measurements and assessing absorption anomaly. *IEEE Trans. Geosci. Remote Sens.,* **42,** 2594–2599.

Loeb, N. G., N. Manalo-Smith, S. Kato, W. F. Miller, S. K. Gupta, P. Minnis, and B. A. Wielicki, 2003: Angular distribution models for top-of-atmosphere radiative flux estimation from the Clouds and the Earth's Radiant Energy System instrument on the Tropical Rainfall Measuring Mission satellite. Part. 1: Methodology. *J. Appl. Meteorol.*, **42**, 240-265, 2003

Minnis, P., D. R. Doelling,L. Nguyen,W. Miller, and V. Chakrapani 2007: Assessment of the visible channel calibrations of the TRMM VIRS and MODIS on Aqua and Terra. *J. Atmos. Oceanic Technol.* **25**, 385-400.

Morstad, D. L., D. R. Doelling, R. Bhatt, B. Scarino, 2011, The CERES calibration strategy of the geostationary visible channels for CERES clouds and flux products, *2011 SPIE Optics + Photonics Conference*, Aug 2011, San Diego, CA

Sohn, B.-J., S.-H. Ham, and P. Yang, 2009: Possibility of the visible-channel calibration using deep convective clouds overshooting the TTL. *J. Appl. Meteor. Climatol.*, **48**, 2271-2283

Vermote E.F. and Y.J. Kaufman, Absolute calibration of AVHRR visible and near infrared channels using ocean and cloud views, *International Journal of Remote Sensing* **16** (1995) (13), pp. 2317–2340

Xiong, X., 2011: MODIS Reflective Solar Calibration and Uncertainty Assessment. *GISCS GWRG meeting*, Daejon, Korea, March 22-25, 2011. https://gsics.nesdis.noaa.gov/wiki/Development/20110322